
Modeling of BrainMap data

Finn Årup Nielsen and Lars Kai Hansen
Department of Mathematical Modelling
Technical University of Denmark
DK-2800 Lyngby, DENMARK
(*fn,lkhansen*)@imm.dtu.dk

Abstract

We apply machine learning techniques in the form of Gaussian mixture models to functional brain activation data. The dataset was extracted through the WWW interface to the BrainMapTM (Research Imaging Center, University of Texas Health Science Center at San Antonio) neuroimaging database. Modeling of the joint probability structure of activation foci and other database entries (e.g. behavioral domain, modality) enables us to summarize the accumulated body of activation coordinates in the form of a 3D density and allows us to explore issues like the effect of the experimental modality on the resulting brainmap

1 Introduction

Neuroimaging experiments based on positron emission tomography (PET), or functional magnetic resonance imaging (fMRI), are accumulating vast spatio-temporal databases at a rate that calls for new innovative informatics tools. Neuroscience databases are conceptually and physically linked in complex socio-scientific networks of human relations, publications, and funding programs. The neuroinformatics challenge is to organize these networks and make them transparent for the neuroscience community [16]. An important part of neuroinformatics concerns the process of relating different functional neuroimaging studies to each other.

A functional neuroimaging study based on fMRI or PET examines the neural correlate of a mental process as it affects cerebral blood flow, for a recent review see [14]. Under the functional segregation paradigm the brain image consists of activation hot spots that each are related to a cognitive component. When discussing the results of a functional study the observed set of activation foci is compared to foci from other studies reported in the literature most often by simple visual inspection, see e.g. a meta-analysis on visual recognition [5]. Such discussions are naturally driven primarily by the informal neuroscientific insight of the researchers involved. Description of the set of foci can be given in terms of lobes or gyri (e.g. dorsolateral prefrontal cortex) or in terms of an informal set of functional areas (such as visual areas V1, V2, ...). An increasingly popular, formal and quantitative alternative is to report foci positions with reference to the Talairach system [17] — a standardized Euclidean system of reference.

The aim of this work is to explore quantitative and automatic procedures for the comparison and discussion of functional data and in this way to pave the road for objective

meta-analyses. We use self-optimizing machine learning algorithms to model the densities of Talairach coordinates and use VRML (virtual reality modeling language) geometric hypertext tools as interface to the learned models.

The long term goal is a tool which can assist the neuroimaging researcher in quantifying and reporting the information content of a study with respect to the accumulated body of neuroscience.

2 BrainMap

The BrainMap™ database is an extensive collection of papers containing Talairach coordinates from human brain mapping studies maintained by the Research Imaging Center, University of Texas Health Science Center at San Antonio [6, 11]. The access to the database is provided by either a graphical user interface application or a web-based interface, see <http://ric.uthscsa.edu>. The database contains bibliographic information about the paper, formal descriptions of the study (e.g. modality, behavioral domain, response type) and 3D coordinates for the functional activations reported in the Talairach system [17]. BrainMap has been used for meta-analytic modeling under the heading “functional volumes modeling” [8, 7], see also [9, 13]. In [8] the location of the activation foci of the mouth is modeled with a bounding box. The estimation of the mouth area required a manual editing of the specific foci that were included to form the volume of interest. In this contribution we will investigate global patterns of foci found under various activation paradigms and we will use machine learning models with minimal user intervention.

3 Generalizable Gaussian Mixtures

Our primary pattern recognition device will be the Gaussian mixture, see, e.g., [15] for a review. Gaussian mixture models have been used in single study functional neuroimaging before, see e.g. [4]. The Gaussian mixture density of a datavector \mathbf{x} , is defined as

$$\begin{aligned}
 p(\mathbf{x}|\boldsymbol{\theta}) &= \sum_{k=1}^K P(k)p(\mathbf{x}|k) \\
 p(\mathbf{x}|\boldsymbol{\theta}_k) &= \frac{1}{\sqrt{|2\pi\boldsymbol{\Sigma}_k|}} \exp\left(-\frac{1}{2}(\mathbf{x} - \boldsymbol{\mu}_k)^\top \boldsymbol{\Sigma}_k^{-1}(\mathbf{x} - \boldsymbol{\mu}_k)\right)
 \end{aligned} \tag{1}$$

where the component Gaussians are mixed with proportions $\sum_k P(k) = 1$, and we have defined the parameter vector $\boldsymbol{\theta} \equiv \{\boldsymbol{\Sigma}_k, \boldsymbol{\mu}_k\}$. The parameters are estimated from a set of examples $D = \{\mathbf{x}_n | n = 1, \dots, N\}$. In the pattern recognition literature mixture densities are mostly estimated by maximum likelihood (ML), using various estimate-maximize (EM) methods [15]. The (negative log-)likelihood costfunction is defined by

$$\mathcal{E}(D; \boldsymbol{\theta}) = \sum_n -\log p(\mathbf{x}_n | \boldsymbol{\theta}) \tag{2}$$

and is minimize by the ML parameters. The Gaussian mixture model is extremely flexible and simply minimizing the above costfunction will lead to an “infinite overfit”. It is easily verified that the costfunction has a trivial (infinite) minimum attained by setting $\boldsymbol{\mu}_k = \mathbf{x}_k$ for $k = 1, \dots, K - 1$, and letting the corresponding covariances shrink to the zero matrix, while the remaining K 'th Gaussian is adapted to the ML fit of the remaining $N - K + 1$ datapoints. This solution is optimal for the training set, but unfortunately has a generalization error roughly equal to that of the single “background” Gaussian. To see this, let the

generalization error is defined as the limit

$$\Gamma(\boldsymbol{\theta}) = \lim_{N \rightarrow \infty} \sum_{n=1}^N -\log p(\mathbf{x}_n | \boldsymbol{\theta}). \quad (3)$$

The ML mixture adapted on a finite dataset has a generalization error where the singular components do not contribute because the data points assigned to the singular datapoints in the training set together have zero measure. This instability has led to much confusion in the literature and needs to be addressed carefully. Basically, there is no way to distinguish generalizable from non-generalizable solutions, if we only consider the likelihood function. The most common fix is to bias the component distributions so that they have a common covariance matrix, see e.g. [10]. Here we have decided to combine three approaches to ensure generalizability. First, we compute centers and covariances on different resamples of the data sets. Secondly, we make an exception rule for sparsely populated components — the covariance matrix defaults to the scaled full-sample covariance matrix. Finally we estimate the number of mixture components using the AIC criterion [1].

The algorithm which is a modified EM procedure [2], and is defined as follows for given K .

Algorithm: Generalizable Gaussian Mixture

Initialization

1. Compute the mean vector $\boldsymbol{\mu}_0 = N^{-1} \sum_n \mathbf{x}_n$.
2. Compute the covariance matrix of the data set: $\boldsymbol{\Sigma}_0 = N^{-1} \sum_n (\mathbf{x}_n - \boldsymbol{\mu}_0)(\mathbf{x}_n - \boldsymbol{\mu}_0)^\top$.
3. Initialize $\boldsymbol{\mu}_k \sim \mathcal{N}(\boldsymbol{\mu}_0, \boldsymbol{\Sigma}_0)$.
4. Initialize $\boldsymbol{\Sigma}_k = \boldsymbol{\Sigma}_0$.
5. Initialize $P(k) = 1/K$.

Repeat until convergence

1. Compute $p(k|\mathbf{x}_n)$ and assign \mathbf{x}_n to the most likely component.
2. Split the data set in two equal parts D_μ, D_Σ .
3. For each k estimate $\boldsymbol{\mu}_k$ on the points in D_μ assigned to component k .
4. For each k estimate $\boldsymbol{\Sigma}_k$ on the points in D_Σ assigned to component k . If the number of datapoints assigned to the k 'th component is less than the dimension, let $\boldsymbol{\Sigma}_k = c \cdot \boldsymbol{\Sigma}_0$, where c is determined so that the total variance of the component corresponds to the variance of the datapoints associated with it.
5. Estimate $P(k)$ as the frequency of assignments to component k .

3.1 Generalizable Gaussian mixture classifier

In pattern recognition we are interested in the joint density of patterns \mathbf{x} and class labels c , denoted by $p(\mathbf{x}, c)$

$$p(\mathbf{x}, c) = p(\mathbf{x}|c)P(c) \quad (4)$$

where $p(\mathbf{x}|c)$ is the class conditioned density and $P(c)$ is the marginal class probabilities. For a labeled dataset we design the classifier by adapting GGM's to each class separately. Hence, the joint density can be written

$$p(\mathbf{x}, c) = \sum_{k=1}^{K_c} p(\mathbf{x}|k)P(k|c)P(c), \quad (5)$$

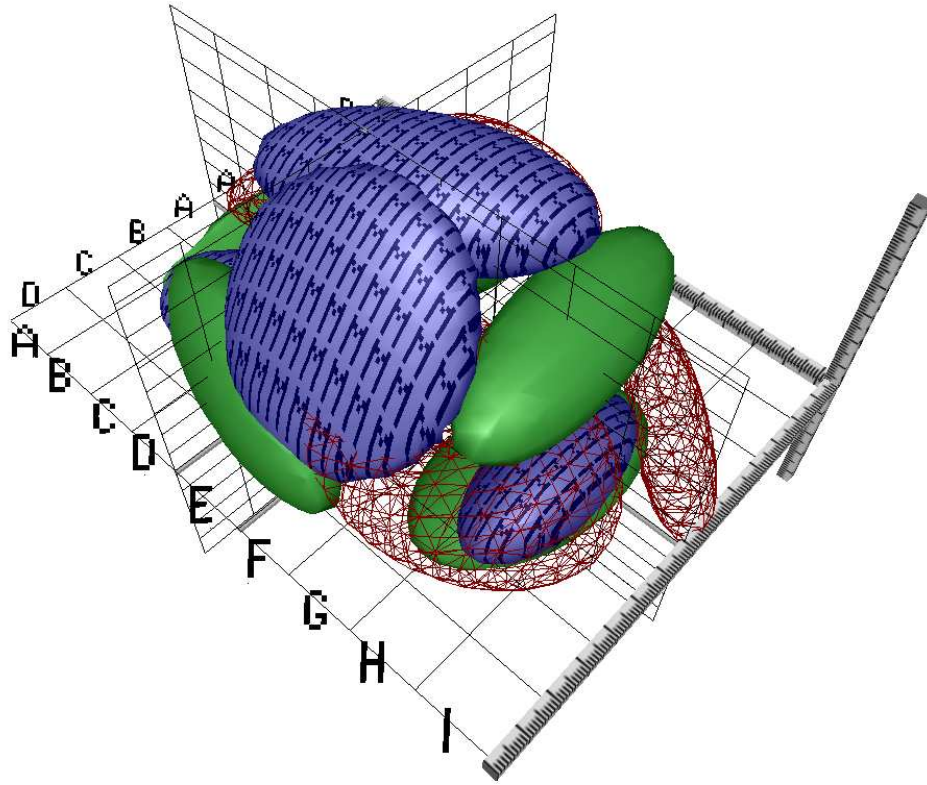


Figure 1: VRML screen shot (from the left side of the back of the brain) of the GGM model from the analysis of the effect of the behavioral domain. It shows isosurfaces in 3 class-conditional densities $p(\mathbf{x}|c)$. The wireframes correspond to the behavioral domain denoted perception in BrainMap, the surfaces to cognition apart from “M” textured surfaces being motion.

where $P(k|c)$ and K_c are the component frequencies and number components found for class c .

4 Results

We downloaded the entire paper and experiment webpages from the BrainMap homepage containing experiment variables and Talairach coordinates denoted locations. The front page of the web interface states that there are 225 papers, 771 experiments and 7683 locations. To each of the locations corresponds a modality, i.e., the type of scanner used to acquire the data. Furthermore, each location has one or more behavioral domains: Perception, cognition, motion, disease, drug and emotion. We used only the first behavioral domain in the list and confined us to the three classes: perception, cognition and motion. (For some of the experiments the modality and behavioral domain was not reported in the database and in the preliminary experiments reported here we simply excluded locations from these experiments.) While modeling the density of locations we found that some of the locations were strong outliers. Some of these foci were probably erroneous entries with decimal point errors. When excluding all locations from papers containing outliers or missing behavioral domain and modality we are left with approximately 3800

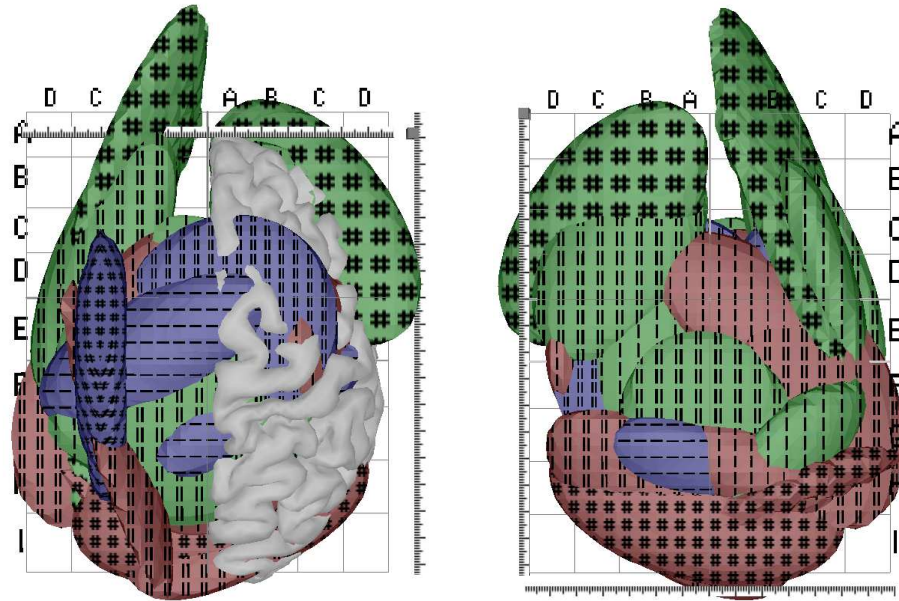


Figure 2: VRML screen shot from the top (left panel) and the bottom (right panel) of the brain. The frontal brain is up in the image. The red surfaces correspond to the behavioral domain denoted perception, the green to cognition and the blue being motion. Textured surfaces with # are derived from the density of fMRI locations, - are PET locations and = are PET-MRI locations. For visual guidance and reference we have included in the left panel also a surface reconstruction of the right cortex of the Visible Man [3].

Talairach coordinates.

We applied the GGM on the BrainMap data with the 3D Talairach coordinates as \mathbf{x} and the modality or behavioral domain represented by label c . In figure 1 is shown the isosurface in the class-conditional densities $p(\mathbf{x}|c)$ for $c \in \{\text{perception, cognition, motion}\}$. A characteristic in this view is the motion cluster in the left hemisphere (as e.g., compared to the right hemisphere) probably stemming from the popular use of the right hand in studies.

In a second experiment we combined behavioral domain and modality for the labels, i.e. with 9 classes in total. Figure 2 shows that the frontal part of the brain is dominated by the conjunction of cognitive and fMRI. We can only speculate about this: Differing spatial normalization procedures or fMRI motion artifacts could have affected the images or the fMRI scanner could be more sensitive in the frontal part. PET dominates in the inferior part of the brain, perhaps explainable by a smaller sensitivity of fMRI in the inferior parts of the brain, e.g., in the frontal regions due to susceptibility distortions.

The generalization in terms of label prediction is not high, which is due to the high overlap between classes:

	Test set rates	Base line probability	
Modality	0.17	0.16	
Behavior	0.47	0.52	(Figure 1)
Modality+Behavior	0.52	0.56	(Figure 2)

With the density model at hand we are able to pick a new functional neuroimaging study and automatically label the activation foci and give the amount of novelty in the experiment

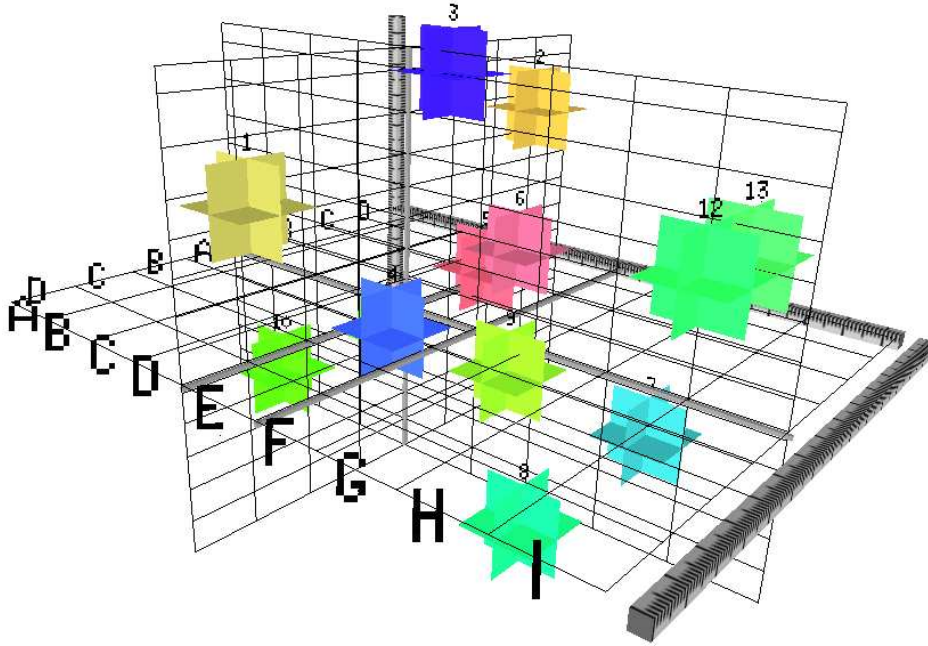


Figure 3: VRML Screen shot of a part of the results from [12]. The glyphs have been colored according to the posterior probability: The red component denote high probability for perception, green component for cognition, and blue component for motion.

(in fact, one location outlier was discovered in this way). In figure 3 is shown the results when the density model with labels from behavioral domain is applied on a saccadic eye-movement experiment [12]. The activation foci reported in the paper have automatically been labeled by the GGM model and the three components of the posterior probabilities have been piped to the red, green and blue color component. The highest posterior probability for a single behavioral domain is the third focus with the most probable label being motion. In the paper the foci has been denoted as the supplementary eye field, — an area associated with the control of eye movements.

5 Conclusion

Machine learning methods can assist the neuroscientists in quality control and provide context by summarizing large neuroimaging databases.

Acknowledgments

We thank Research Imaging Center, University of Texas Health Science Center at San Antonio for access to the BrainMap database. This paper has been supported by the Danish research councils through “THOR center for Neuroinformatics” and “Interdisciplinary Neuroresearch” and the American NIH “Human Brain Project” grant R01 DA09246 and P20 MH57180.

References

- [1] H. Akaike. A new look at the statistical model identification. *IEEE Transactions on Automatic Control*, 19:716–723, 1974.
- [2] A. P. Dempster, N. M. Laird, and D. B. Rubin. Maximum likelihood from incomplete data via the EM algorithm. *Journal of the Royal Statistical Society, Series B*, 39:1–38, 1977.
- [3] Heather A. Drury and David C. Van Essen. *CARET User's Guide*. Washington University School of Medicine, St. Louis, Missouri, USA, September 1997.
- [4] Brian S. Everitt and Edward T. Bullmore. Mixture model mapping of brain activation in functional magnetic resonance images. *Human Brain Mapping*, 7(1):1–14, 1999.
- [5] Martha J. Farah and Geoffrey K. Aguirre. Imaging visual recognition: PET and fMRI studies of the functional anatomy of human visual recognition. *Trends in Cognitive Sciences*, 3(5):179–186, May 1999.
- [6] Peter T. Fox and Jack L. Lancaster. Neuroscience on the net. *Science*, 266(5187):994–996, November 1994.
- [7] Peter T. Fox, Jack L. Lancaster, Lawrence M. Parson, Jin-Hu Xiong, and Frank Zarnarripa. Functional volumes modeling: Theory and preliminary assessment. *Human Brain Mapping*, 5(4):306–311, 1997.
- [8] Peter T. Fox, Jack L. Lancaster, Lawrence M. Parsons, and Jin-Hu Xiong. Functional volumes modeling: Metanalytic models for statistical parametric imaging. In Lars Friberg, Albert Gjedde, Søren Holm, Niels A. Lassen, and Markus Nowak, editors, *Third International Conference on Functional Mapping of the Human Brain, NeuroImage*, volume 5, page S397. Academic Press, May 1997.
- [9] Peter T. Fox, Lawrence M. Parsons, and Jack L. Lancaster. Beyond the single study: functional/location metanalysis in cognitive neuroimaging. *Current Opinion in Neurobiology*, 8(2):178–187, April 1998.
- [10] Trevor Hastie and Robert Tibshirani. Discriminant analysis by Gaussian mixtures. *Journal of the Royal Statistical Society, Series B, Methodology*, 58(1):155–176, 1996.
- [11] Jack L. Lancaster, Peter T. Fox, Gwendolyn Davis, and Shawn Mikiten. BrainMap: A database of human functional brain mapping. In *The Fifth International Conference: Peace through Mind/Brain Science*, Hammamatsu, Japan, February 1994.
- [12] Ian Law, Claus Svarer, Egill Rostrup, and Olaf B. Paulson. Parieto-occipital cortex activation during self-generated eye movements in the dark. *Brain*, 121(11):2189–2200, November 1998.
- [13] M. Lepage, R. Habib, and E. Tulving. Hippocampal PET activations of memory encoding and retrieval: The HIPER model. *Hippocampus*, 8(4):313–322, 1998.
- [14] Michael I. Posner and Marcus E. Raichle. *Images of Mind*. Scientific American Library, 1997.
- [15] Brian D. Ripley. *Pattern Recognition and Neural Networks*. Cambridge University Press, 1996.
- [16] Gordon M. Shepherd, Jason S. Mirsky, Matthew D. Healy, Michael S. Singer, Emmanouil Skoufos, Michael S. Hines, Parkash M. Nadkarni, and Perry L. Miller. The Human Brain Project: neuroinformatics tools for integrating, searching and modeling multidisciplinary neuroscience data. *Trends in Neurosciences*, 21(11):460–468, November 1998.
- [17] J. Talairach and P. Tournoux. *Co-planar Stereotaxic Atlas of the Human Brain*. Thieme Medical Publisher Inc, New York, 1988.